Unimolecular Decomposition of the Anionic Form of N-Chloro-α-glycine. A Theoretical Study

ARTICLE *in* THE JOURNAL OF PHYSICAL CHEMISTRY · FEBRUARY 1996

Impact Factor: 2.78 · DOI: 10.1021/jp9517209

Unimolecular Decomposition of the Anionic Form of *N*-Chloro-α-glycine. A Theoretical Study

J. Andrés,* J. J. Queralt, and V. S. Safont

Departament de Ciències Experimentals, Universitat Jaume I, Box 242, E-12080 Castelló, Spain

M. Canle L. and J. A. Santaballa

Departamento de Química Fundamental e Industrial, Facultade de Ciencias, Universidade da Coruña, A Zapateira, s/n. E-15071 A Coruña, Spain

Received: June 20, 1995; In Final Form: September 13, 1995[⊗]

The molecular mechanism for the unimolecular decomposition of the anionic form of *N*-chloro-α-glycine in its singlet and triplet electronic states has been theoretically characterized by using analytical gradients and AM1 and PM3 semiempirical procedures as well as the *ab initio* RHF and UHF methods at 4-31G, 6-31G*, and 6-311+G* basis set levels. Correlation effects were included by using the perturbational approach at the MP2/6-31G* level. The global potential energy surfaces have been further studied, and the stationary points were localized and characterized. The geometry, electronic structure, and the transition vector associated with the transition structures have been analyzed. The dependence of these properties upon theoretical methods is analyzed and discussed. The topological analysis of the fundamental singlet and triplet PESs shows the existence of a quadratic flat region that plays a fundamental role in the description of the nature of the molecular mechanism. The decomposition process takes place in the singlet electronic state. The geometry and electronic structure for TSs in singlet and triplet states correspond to antiperiplanar conformations, possessing a productlike character. The unimolecular decomposition mechanism is a concerted and slightly asynchronous process.

1. Introduction

Water chlorination is one of the methods most widely used for disinfection purposes. Its drawback is the formation of a wide range of chlorinated byproducts, some of them with carcinogenic and/or mutagenic properties.[1,2] *N*-chloro-α-amino acids are found after chlorination of natural waters. These compounds are unstable in aqueous solution, decomposing readily to carbon dioxide, a chloride ion, ammonia, and a carbonyl compound possessing one fewer carbon atom (Strecker degradation).[3] The mechanism of this chlorination/decomposition process has three steps, the second one being the rate-limiting step:[4]

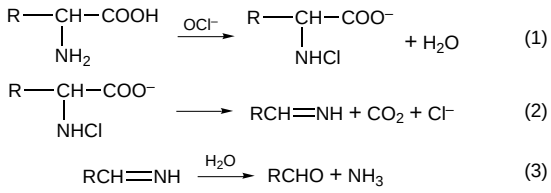

Several studies have focused on the stability of *N*-chloro-α-amino acids in aqueous solution in acidic conditions similar to those of natural waters, and a great amount of energy and rate data are available; however, the precise nature of the mechanism remains the subject of some controversy.[4−13]

Determination of molecular reaction mechanism has always been of major interest in theoretical and physical chemistry, the transition state theory being a fairly successful method to describe chemical reactions.[14,15] In this theory, the molecular mechanism of a given chemical reaction is defined by the transition structure (TS) associated with the chemical interconversion step. From a theoretical point of view, the region around the TS on the potential energy surface (PES),[16] *i.e.*, the quadratic zone, connects the valleys of reactants and products and leads the reaction kinetic data. For a given mechanism, if the corresponding PES has a TS with a transition vector (TV)[17] displaying the reactive fluctuation pattern of the particular chemical interconversion step, then the relevant structural and dynamic information resides in the quadratic zone of the TS.

Nowadays, the application of quantum mechanical techniques to the determination of PES representing the chemical reaction is well accepted.[18] Increasing computer power, software, and advances in theory have provided powerful tools for understanding and describing reactions, especially in cases where experimental determination is uncertain. The results of such calculations can be used to examine the validity of hypothetical mechanistic pathways, to determine the relative importance of several structural factors on reactivity, and to predict the outcomes of reactions.

Although many experimental data are available from our works,[5] no theoretical computations have been devoted to the study of the *N*-chloro-α-amino acids unimolecular decomposition mechanism. As a part of a more extensive research project on the reactivity of the *N*-halo derivatives, a theoretical study of the unimolecular decomposition of *N*-chloro-α-amino acids in gas phase using semiempirical and *ab initio* methods has been carried out.

The present study is organized as follows: the molecular model and computing methods are briefly described in section 2. A variety of approaches is used, and we assess the quality of the main calculations on the basis of the consistency and comparison between different methods. In order to characterize the nature of the decomposition process, the energy, the geometries of stationary points on PES (reactant and TS), and the evolution of the bond orders and charge distribution along the reaction pathway are discussed and analyzed for the system in its singlet and triplet electronic states in section 3. Finally, our main conclusions close this paper.

[⊗] Abstract published in *Advance ACS Abstracts,* December 15, 1995.

0022-3654/96/20100-3561$12.00/0

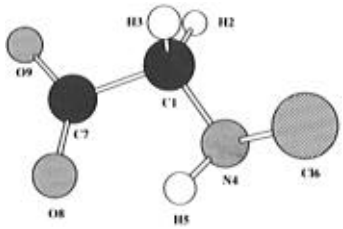

Figure 1. Numbering of the atoms for the anionic form of *N*-chloro-α-glycine model (**I**).

2. Computational Methods and Model

All calculations were carried out using the GAUSSIAN 92 package[19] on an IBM RISC/6000 workstation. We started by characterizing the whole PES in both the fundamental singlet and the first excited triplet states at PM3[20,21] and AM1[22] semiempirical levels. Both methods derive from the same theoretical framework; *i.e.*, they use the same basic approximations (MO-LCAO HF combined with the NDDO approximation[23]) and differ mainly in the way in which they are parametrized. In the AM1 procedure, additional Gaussian terms occur in the core repulsion function defined in the MNDO with the aim of correcting the excessively long-range core−core repulsions, whereas in the PM3 level a new technique for obtaining optimized parameters is applied.[24,25] Semiempirical methods have progressed over the past few years to a surprising level of accuracy and reliability, considering the limitations of the underlying approximations.[26−28]

The *ab initio* calculations have been performed at HF/4-31G, HF/6-31G*, and HF/6-311+G* basis set levels. Electron correlation energy has been included by using the second-order MP2 perturbation theory[29] at the 6-31G* level. The comparative analysis of the results obtained with the different methods can be used to look for a computational method which is an adequate compromise between accuracy and computing time.

Different glycine conformers and their relative energies have been thoroughly characterized using *ab initio* calculation with standard schemes: restricted Hartree−Fock (RHF) for the singlet state and unrestricted Hartree−Fock (UHF) for the triplet,[30,31] at different basis set levels.[32−36] A previous study has shown that the fact of choosing one conformer or another has very little effect in the PES calculation. The selected model is the most simple representative of *N*-chloro-α-amino acids, *i.e.*, *N*-chloro-α-glycine in its anionic form $ClHN-CH_2-COO^-$ (**I**). This model compound is somewhat simpler than the compounds used experimentally but likely embodies the important features for this discussion. The emphasis is on the investigation of the effect of the computational method on the structures and energy status of stationary points. The relatively small size of the system makes possible to use extensive and flexible basis sets with reasonable computational time and economy. Reactant geometry and atom numbering for the selected model are depicted in Figure 1.

The PESs in singlet and triplet electronic states have been calculated in considerable detail by using semiempirical procedures, locating the relevant stationary points. The unimolecular decomposition implies the formation of a double bond from a single one, C1−N4, and the cleavage of two bonds: C1−C7 and N4−C16. These latter are used to characterize the PES and they were changed stepwise, 0.1 Å, from reactants to products, except in TS zone where they were changed by steps of 0.01 Å. In every point all relevant degrees of freedom were submitted to optimization.

Geometries were optimized with the help of the Berny analytical gradient optimization routines.[37,38] The requested convergence on the density matrix was 10^{-9} atomic units, and the threshold value of maximum displacement was 0.0018 Å and that of maximum force was 0.000 45 hartree/bohr. For the triplet state, low levels of spin contamination were found. Typical values for the spin squared range between 2.0001 and 2.005.

TS searching was performed within all calculation levels with an "eigenvalue following" optimization method.[39,40] The nature of a particular stationary point on the PES was confirmed by the number of imaginary frequencies. All TSs possessed only one imaginary frequency, while all minima had none.

3. Results and Discussion

3.1. Energetics. The energetic results for the stationary points obtained with the different levels of calculation are reported in Table 1. The singlet state has lower energy than the triplet state in all stationary points found, except in the reactant zone when calculations are made at the 4-31G level, concluding that the reaction path is developed via the fundamental singlet state. The activation barrier calculated by using the semiempirical methods ranges between 24 and 26 kcal/mol. The results with *ab initio* method without correlation diminishes this value to a range between 17 and 20 kcal/mol. The correlation energy plays an important role in this process, where there are breaking/making bonds. In fact, the inclusion of correlation energy at the MP2/6-31G* level further reduces the energy barrier to 11 kcal/mol.

For the *N*-chloro-α-glycine, very different values for the rate constant, ranging from *ca.* 10^{-4} to *ca.* 10^{-6} s^{-1}, can be found in the literature;[41] nevertheless, it is always found that this reaction is spontaneous, and then the barrier height would be small. We cannot make a comparison between experimental

TABLE 1: Heat of Formation (au) for Semiempirical Methods and Total Energy (au) of Reactants (I) and TS for the Decomposition Process of the Anionic Form of *N*-Chloro-α-glycine in Gas Phase (Singlet and Triplet States) Obtained at different Levels of Calculation; Relative Energy in kcal/mol in Parentheses

	singlet		triplet	
	I	TS	**I**	TS
AM1	−0.167 875	−0.126 215	−0.135 243	−0.089 022
	(0.0)	(26.14)	(20.48)	(49.48)
PM3	−0.199 237	−0.160 474	−0.158 425	−0.115 403
	(0.0)	(24.32)	(25.61)	(52.61)
HF/4-31G	−740.216 957	−740.188 752	−740.218 327	−740.170 545
	(0.0)	(17.70)	(−0.86)	(29.12)
HF/6-31G*	−741.129 174	−741.099 844	−741.113 981	−741.068 734
	(0.0)	(18.44)	(9.53)	(37.92)
HF/6-311+G*	−741.244 256	−741.211 608	−741.228 171	−741.187 395
	(0.0)	(20.49)	(10.09)	(35.68)
MP2/6-31G*	−742.067 191	−742.049 154	−742.007 898	−741.942 128
	(0.0)	(11.32)	(37.21)	(78.48)

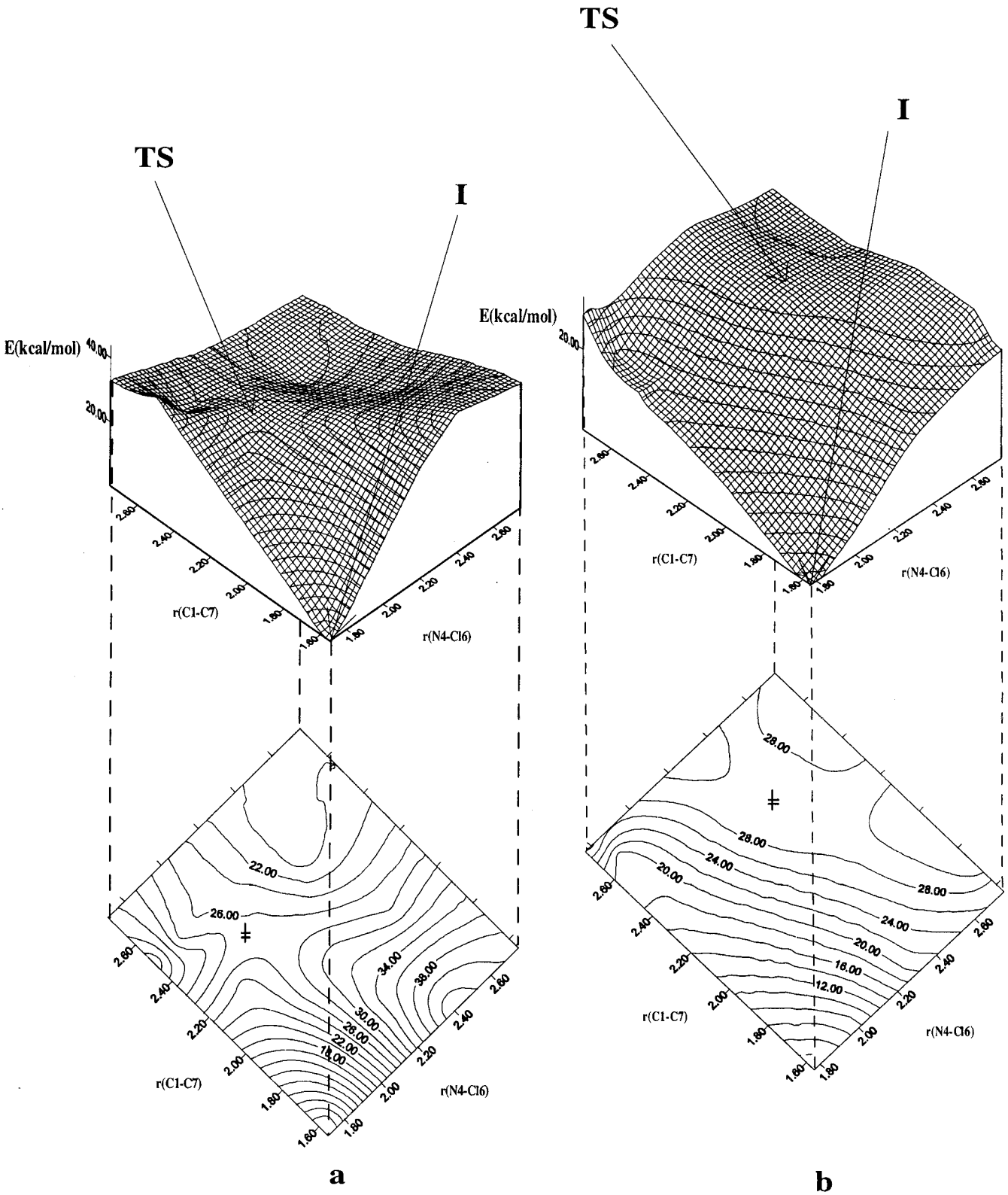

Figure 2. PES and energy map for the unimolecular decomposition of the fundamental singlet (a) and first excited triplet (b) electronic states calculated with the AM1 method. Relative energies (in kcal/mol) are represented as a function of C1−C7 and N4−Cl6 bond distances. In each surface, the reference point is the energy of the reactant in the corresponding electronic state.

values and our theoretical results, the activation energy of the reaction being extremely sensitive to electron correlation effects. Deciding the level necessary for an accurate description of a reaction energy surface is still a demanding task; the second-order perturbation treatment is known to account for about 90% of the basis set correlation energy,[42] but it is also known that MP2 calculations overcorrect the HF result in the case of activation energies.[43]

In the triplet state, the TS relative energy to the fundamental singlet state reactant is in all cases higher than in singlet state: when using semiempirical methods, we found values between 49 and 52 kcal/mol, while the values are in the interval between 29 and 35 kcal/mol at the *ab initio* level, and the inclusion of correlation energy raises this value to 78 kcal/mol. The energetic difference between TS and **I**, both in its first excited triplet state, ranges between 27 and 29 kcal/mol at the

TABLE 2: Relevant Geometric Parameters for I at Different Levels of Calculation in Singlet State[a]

	AM1	PM3	HF/4-31G	HF/6-31G*	HF/6-311+G*	MP2/6-31G*
r(C1−N4)	1.452	1.469	1.464	1.460	1.460	1.465
r(N4−Cl6)	1.714	1.754	1.890	1.762	1.755	1.783
r(C1−C7)	1.555	1.565	1.556	1.560	1.556	1.568
r(C7−O9)	1.260	1.250	1.243	1.225	1.224	1.252
r(C1−H3)	1.121	1.106	1.082	1.087	1.088	1.099
r(C1−H2)	1.127	1.106	1.076	1.082	1.081	1.093
r(C7−O8)	1.264	1.256	1.257	1.236	1.232	1.268
r(N4−H5)	1.015	1.002	1.007	1.004	0.999	1.033
∠(H2−C1−H3)	107.93	106.81	108.90	108.15	108.22	108.31
∠(H5−N4−Cl6)	102.73	106.99	102.87	104.88	105.19	104.46
∠(C1−C7−O9)	116.82	117.71	114.88	114.54	114.61	115.19
∠(N4−C1−C7)	116.17	114.92	108.33	109.06	109.78	107.53
∠(O8−C7−O9)	125.27	123.86	130.26	130.76	130.32	130.81
∠(C1−N4−Cl6)	112.67	111.48	111.49	112.58	112.25	111.77
∠(C1−C7−O8)	117.91	118.42	114.80	114.63	115.01	113.92

[a] Distances (*r*) in angstroms and angles (∠) in degrees.

TABLE 3: Relevant Geometric Parameters for I at Different Levels of Calculation in Triplet State

	AM1	PM3	HF/4-31G	HF/6-31G*	HF/6-311+G*	MP2/6-31G*
r(C1−N4)	1.415	1.423	1.443	1.436	1.436	1.429
r(N4−Cl6)	1.778	1.901	2.329	2.324	2.326	2.293
r(C1−C7)	1.561	1.576	1.552	1.563	1.559	1.574
r(C7−O9)	1.258	1.246	1.244	1.223	1.222	1.249
r(C1−H3)	1.127	1.107	1.082	1.086	1.085	1.098
r(C1−H2)	1.127	1.107	1.082	1.086	1.085	1.098
r(C7−O8)	1.262	1.253	1.256	1.234	1.231	1.267
r(N4−H5)	1.000	0.987	1.012	1.012	1.007	1.039
∠(H2−C1−H3)	107.11	106.05	107.11	106.74	106.59	106.15
∠(H5−N4−Cl6)	118.35	119.24	121.80	121.21	119.91	124.21
∠(C1−C7−O9)	116.05	117.21	114.84	114.07	114.00	114.51
∠(N4−C1−C7)	115.68	114.77	111.72	111.90	112.18	110.51
∠(O8−C7−O9)	125.83	125.05	130.47	131.44	131.01	131.67
∠(C1−N4−Cl6)	126.06	120.96	125.65	127.86	127.41	128.23
∠(C1−C7−O8)	118.12	117.74	114.69	114.49	114.99	113.82

semiempirical level and between 25 and 30 kcal/mol at the *ab initio* level, and at the MP2/6-31G* level, the energetic difference is 41 kcal/mol. Barrier heights in the triplet state are always larger than in the singlet state; this fact supports that the mechanism via the triplet electronic state can be discarded in the gas phase.

In Figure 2a,b, two- and three-dimensional surface contours for the unimolecular decomposition process obtained at the AM1 semiempirical level are presented for singlet and triplet states, respectively. The shapes of both PES show a central channel corresponding to the reaction pathway connecting the stationary points representing **I** and TS. The molecular mechanism would correspond to a concerted process either in singlet or in triplet states. Motion through a stepwise mechanism from the reactants to the upper-left or lower-right corners, representing carbanion-like or nitrenium-like species, respectively, can be discarded. A similar topology for these PES has been found at the PM3 semiempirical level. These theoretical results are in agreement with recent experimental data.[5]

3.2. Geometries. The geometric parameters for **I** in its singlet and triplet states are reported in Tables 2 and 3, respectively. In Table 2 some minor differences can be detected between the results obtained by using the two semiempirical procedures and the results obtained with *ab initio* calculations. Mainly, both distances C1−H3 and C1−H2 are predicted to be a little larger by the semiempirical procedures, and differences ranging between 1° and 8° can be noticed in the bond angles. Among the *ab initio* results, those obtained with the 4-31G basis set show some small differences in relation to the others, for instance in the N4−Cl6 and C7−O8 distances and in the H5−N4−Cl6 bond angle. As for the triplet state, it may be observed that with *ab initio* methods the value for the N4−Cl6 bond length is predicted to be about 0.4 Å larger than that obtained with semiempirical calculations. In spite of these minor differences, it can be seen that in all methods the geometries of **I** in its singlet and triplet states are fairly invariant.

The geometric parameters for TS in singlet and triplet states are listed in Tables 4 and 5, respectively. In the singlet state, the main difference lies in the results of C1−C7 and N4−Cl6 distances obtained with semiempirical and *ab initio* methods. The C1−C7 bond distance is found to be larger at the semiempirical level than when using the *ab initio* method; however, the N4−Cl6 bond distance presents larger values with *ab initio* calculations. Some other differences were found in the values of O8−C7−O9, C1−C7−O9, and C1−C7−O8 bond angles between the semiempirical and the *ab initio* results. In particular, the N4−C1−C7 angle obtained by means of PM3 method presents the highest value.

In triplet state some differences can be detected. The C1−C7 bond distance value increases when the *ab initio* procedure is used and correlation effects are taken into account. The C1−N4 bond distance is shorter, and MP2/6-31G* also increases this effect. The C7−O8 and C7−O9 bond distances present a higher value at HF/4-31G and MP2/6-31G* levels. There are several important differences for bond angles: H5−N4−Cl6 is lower at the AM1 procedure; C1−C7−O9 value ranges between 85° (MP2/6-31G*) and 103° (PM3); for the C1−C7−O8, the values range between 98° (AM1) and 139° (MP2/6-31G*); for the O8−C7−O9, the values range between 152−164° and 136−139° for semiempirical and *ab initio* methods, respectively.

TS geometry in singlet and triplet states are depicted in Figures 3 and 4, respectively. It can be seen that both conformations are antiperiplanar in relation to the chlorine center, Cl6, and C7. The C7−C1−N4−Cl6 dihedral angle

TABLE 4: Geometrical Parameters for the TS in Singlet State Calculated with the Different Methods

	AM1	PM3	HF/4-31G	HF/6-31G*	HF/6-311+G*	MP2/6-31G*
r(C1−N4)	1.311	1.320	1.339	1.347	1.344	1.358
r(N4−Cl6)	2.086	2.060	2.331	2.249	2.253	2.129
r(C1−C7)	2.358	2.380	1.926	1.833	1.831	1.841
r(C7−O9)	1.197	1.189	1.204	1.193	1.189	1.225
r(C1−H3)	1.103	1.090	1.078	1.083	1.083	1.097
r(C1−H2)	1.101	1.087	1.069	1.076	1.075	1.089
r(C7−O8)	1.198	1.190	1.210	1.199	1.194	1.229
r(N4−H5)	1.005	0.989	1.003	1.002	0.999	1.025
∠(H2−C1−H3)	114.59	114.56	115.15	114.16	114.47	113.30
∠(H5−N4−Cl6)	87.57	92.65	81.59	86.20	86.69	90.75
∠(C1−C7−O9)	97.42	99.50	107.78	108.87	108.77	108.99
∠(N4−C1−C7)	96.86	104.04	99.33	99.10	98.48	99.62
∠(O8−C7−O9)	164.29	161.01	142.70	140.82	140.80	140.73
∠(C1−N4−Cl6)	114.92	112.30	110.58	111.24	111.02	112.91
∠(C1−C7−O8)	98.19	99.43	109.38	110.17	110.29	110.12

TABLE 5: Geometrical Parameters for the TS in the First Triplet State Calculated with the Different Methods

	AM1	PM3	HF/4-31G	HF/6-31G*	HF/6-311+G*	MP2/6-31G*
r(C1−N4)	1.331	1.341	1.286	1.275	1.278	1.254
r(N4−Cl6)	2.326	2.536	2.349	2.363	2.370	2.325
r(C1−C7)	2.319	2.151	2.521	2.587	2.538	2.796
r(C7−O9)	1.198	1.200	1.239	1.219	1.207	1.259
r(C1−H3)	1.106	1.093	1.070	1.074	1.074	1.074
r(C1−H2)	1.100	1.093	1.067	1.073	1.073	1.073
r(C7−O8)	1.197	1.198	1.228	1.208	1.201	1.240
r(N4−H5)	0.988	0.978	1.000	1.002	1.002	1.002
∠(H2−C1−H3)	116.09	113.09	116.95	117.09	117.32	117.06
∠(H5−N4−Cl6)	91.39	116.00	113.71	115.16	115.20	114.14
∠(C1−C7−O9)	97.72	103.02	95.36	93.06	98.98	84.57
∠(N4−C1−C7)	115.00	115.00	120.61	124.35	120.00	118.25
∠(O8−C7−O9)	164.29	152.55	137.70	138.16	139.64	136.25
∠(C1−N4−Cl6)	125.00	125.00	125.83	128.08	128.03	128.08
∠(C1−C7−O8)	97.88	104.43	126.74	128.73	120.94	139.11

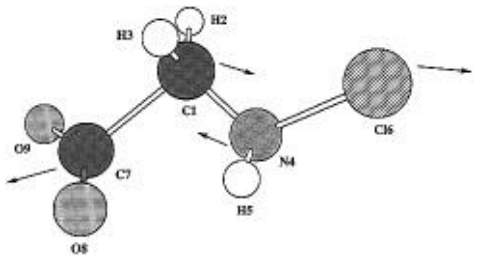

Figure 3. TS for the decomposition process of the anionic form of **I** in its fundamental singlet state, calculated at the MP2/6-31G* theoretical level. Arrows indicate the main atom motions corresponding to the vibration of the imaginary frequency.

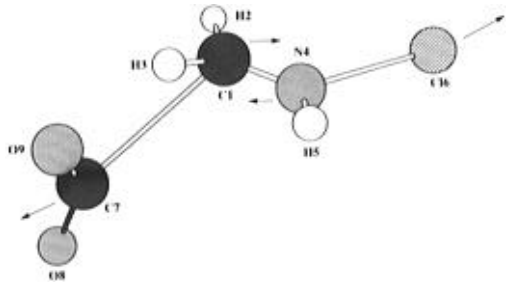

Figure 4. TS for the decomposition process of the anionic form of **I** in the first excited triplet state, calculated at the MP2/6-31G* theoretical level.

presents values around 160° and 130° for singlet and triplet states, respectively. This geometry provides a great overlap of π-orbitals to yield the C1−N4 double bond.

The unique negative eigenvalue from the diagonalization of the Hessian, the imaginary frequency, the force constants for those selected geometric parameters with nonzero components in the TV,[17] and corresponding components of the eigenvector in this control space have been listed in Tables 6 and 7 for the TS in its singlet and triplet states, respectively. The TV for both TSs yields the essentials of the chemical process under study. The control space contains internal variables that define the chemical interconversion process. There are two dominant contributions, which are fairly invariant to the method used, as shown by a perusal of the amplitudes of the TV, *i.e.*, the two bonds, C1−C7 and N4−Cl6, that are broken. The TS is well associated in all cases to the decomposition process. The C1−N4 bond distance, which evolves from single to double bond, has minor participation in the TV, being very low in the triplet state. Together with these three distances, the TV components corresponding to the O8−C7−C1 and O9−C7−C1 angles have also been reported. On the other hand, the O8−C7−C1 and O9−C7−C1 components of the triplet state TV are increased with respect to that of singlet state when *ab initio* calculations are carried out.

The imaginary frequency values are in the range 295−66li and 95−437i cm^{-1} for the TSs in singlet and triplet state, respectively. The normal-mode analysis of these structures yields a relatively low imaginary frequency, indicating that the quadratic zones around TS are flat and associated with the heavy atom motions.

3.3. Bond Orders. In order to calculate the progress of the decomposition process at the TS, Pauling bond orders[44] (BO) were calculated for TSs through the following expression:

$$\mathrm{BO} = \exp\{[R(1) - R(\mathrm{TS})]/0.3\} \qquad (4)$$

where R(TS) represents the length corresponding to a bond in TS and R(1) represents the reference bond length. For the breaking bonds (C1−C7 and N4−Cl(6), the reference values considered were the equilibrium distances in **I**, and for the C1−N4 bond, which evolves from single to double, the reference

TABLE 6: Hessian Unique Negative Eigenvalue (au), Imaginary Frequency (cm^{-1}) Obtained from a Normal Mode Analysis, Force Constants (*F*, au), and Hessian Eigenvector Components (*C*) for the TS in the Singlet State

	AM1		PM3		HF/4-31G		HF/6-31G*		HF/6-311+G*		MP2/6-31G*	
eigenvalue	−0.06366		−0.03783		−0.07626		−0.11033		−0.12601		−0.08256	
imaginary frequency	350.37i		295.44i		543.13i		610.80i		661.04i		465.86i	
	F	*C*	*F*	*C*	*F*	*C*	*F*	*C*	*F*	*C*	*F*	*C*
r(C1−N4)	0.83	−0.11	0.70	−0.12	0.51	−0.20	0.48	−0.23	0.47	−0.24	0.48	−0.19
r(N4−Cl6)	−0.02	0.90	0.03	0.70	0.04	0.56	0.02	0.61	0.01	0.62	0.03	0.65
r(C1−C7)	0.04	0.30	0.02	0.59	0.04	0.67	0.05	0.64	0.05	0.62	0.05	0.62
∠(O8−C7−C1)	0.18	−0.10	0.18	−0.15	0.51	−0.09	0.56	−0.07	0.55	−0.08	0.49	−0.07
∠(O9−C7−C1)	0.17	−0.11	0.18	−0.15	0.47	−0.19	0.50	−0.21	0.49	−0.21	0.43	−0.20

TABLE 7: Hessian Unique Negative Eigenvalue (au), Imaginary Frequency (cm^{-1}) Obtained from a Normal Mode Analysis, Force Constants (*F*, au), and Hessian Eigenvector Components (*C*) for the TS in the First Triplet State

	AM1		PM3		HF/4-31G		HF/6-31G*		HF/6-311+G*		MP2/6-31G*	
eigenvalue	−0.08987		−0.03783		−0.02553		−0.11968		−0.01268		−0.01542	
imaginary frequency	437.69i		220.53i		98.36i		95.25i		127.20i		345.47i	
	F	*C*	*F*	*C*	*F*	*C*	*F*	*C*	*F*	*C*	*F*	*C*
r(C1−N4)	0.72	−0.01	0.60	−0.03	0.62	−0.06	0.67	−0.06	0.63	−0.05	1.12	−0.08
r(N4−Cl6)	0.03	0.79	0.01	0.75	0.05	0.11	0.04	0.10	0.04	0.11	0.06	0.09
r(C1−C7)	0.04	0.14	0.05	0.58	0.01	0.80	0.01	0.82	0.01	0.76	0.02	0.70
∠(O8−C7−C1)	0.16	0.06	0.23	0.18	0.36	0.30	0.36	0.32	0.32	0.32	0.32	0.43
∠(O9−C7−C1)	0.16	0.06	0.21	0.16	0.43	−0.24	0.44	−0.24	0.37	−0.25	0.44	−0.27

TABLE 8: Percentage of Bond Breaking at TS for Equilibrium Length of C1−C7 and N4−Cl6 Bond and Percentage of Bond Making for Equilibrium Length of C1−N4 Double Bond

	C1−C7	N4−Cl6	C1−N4
	Singlet		
AM1	93.0	60.0	87.2
PM3	93.0	64.0	86.4
HF/4-31G	70.8	76.9	92.0
HF/6-31G*	59.3	80.5	72.5
HF/6-311+G*	60.0	81.0	73.1
MP2/6-31G*	60.7	67.8	77.4
	Triplet		
AM1	92.0	83.9	96.5
PM3	85.3	88.0	94.6
HF/4-31G	96.0	6.4	90.6
HF/6-31G*	96.7	12.2	92.2
HF/6-311+G*	96.2	13.5	91.2
MP2/6-31G*	98.3	10.1	95.2

value was the equilibrium length of the double bond in methylimine. Calculated BO in percentages for singlet and triplet TSs are reported in Table 8. At the TS the evolution of the bond cleavage and formation is very advanced, and the TS is productlike. This is in agreement with previous experimental and kinetic work.[41]

A more detailed analysis of this data shows that the methodology employed has great influence on the results obtained. In the singlet state the semiempirical calculations show that in TS the C1−C7 bond has been almost completely broken (93% cleavage); meanwhile, the N4−Cl6 bond has been only cleaved approximately 60%. On the contrary, *ab initio* results show a greater degree for the cleavage of the N4−Cl6 bond (77−81%) than for the C1−C7 bond (59−70%) in all cases. When correlation effects are included, the same trend is observed, the N4−Cl6 bond being more cleaved (68%) than the C1−C7 bond (61%). This would imply a slightly asynchronous mechanism in which the process would be characterized by a cleavage of N4−Cl6 bond accompanied by an important increase of the double-bond character of Cl−N4 (77% of its final bond order), producing a less pronounced cleavage of the C1−C7 bond.

In the triplet electronic state several differences can be detected. Both C1−C7 and N4−Cl6 bonds have a high degree of breaking at the TS (83−92%) at the semiempirical level; however, with the *ab initio* method, with or without inclusion of correlation energy, the N4−Cl6 bond breaking process is predicted to be scarcely developed at the TS (6−13%) while C1−C7 bond also has a high degree of cleavage (96−98%). In the triplet state the decomposition process has a more developed asynchronicity, the C1−C7 cleavage is more advanced than N4−Cl6 breaking, and C1−N4 double bond making is almost completed.

3.4. Atomic Charges. One step further in this analysis implies understanding the electronic distribution change along the reaction path from **I** to TS. For this purpose, a Mulliken atomic population analysis is carried out. Net atomic charges calculated for singlet and triplet states are presented in Tables 9 and 10, respectively. For **I**, an analysis of the results at semiempirical and *ab initio* methods shows differences between net atomic charges on N4, H5, and C7 atomic centers. For TS in singlet and triplet electronic state we can also observe some differences: the C1 atomic center has a minor negative charge at the *ab initio* level, while the N4 atomic center has a greater one. The H5 atomic center has a great positive charge at the *ab initio* level while the C7−O8−O9 group develops an important negative charge at this level.

The net atomic charge evolution from **I** to TS in singlet state corresponds to a heterolytic fragmentation, similar to the (1,2)-elimination processes.[45] As can be expected,[46] the diffuse function (6-311+G*) yields a different charge distribution for **I** and TS, but all methods yield a displacement of the negative atomic charge from the carboxylate (CO_2) to the chlorine (Cl6) fragments, an increment of the negative charge on C1 atom, and an opposite effect on N4 atom along the reaction path **I**−TS. A similar result is obtained by using a natural population analysis (NPA). Otto and Ladik[47] have noted that the charge transfer, measured with Mulliken's population analysis, yields acceptable values while Bertrán *et al.*[48] have found that Mulliken and NPA yield qualitatively the same trend of results.

4. Conclusions

The results presented in this paper are based on the geometry optimization using AM1 and PM3 semiempirical methods and *ab initio* HF/4-31G, HF/6-31G*, and HF/6-311+G* procedures, including correlation effect at the MP2/6-31G* level. We note that there are central issues that we have not been able to address

TABLE 9: Net Atomic Charges for I and TS in Singlet State

	AM1		PM3		HF/4-31G		HF/6-31G*		HF/6-311+G*		MP2/6-31G*	
	I	TS	**I**	TS	**I**	TS	**I**	TS	**I**	TS	**I**	TS
C1	−0.31	−0.52	−0.35	−0.67	−0.21	−0.29	−0.23	−0.29	−0.63	−0.65	−0.23	−0.29
H2	0.14	0.16	0.12	0.17	0.18	0.19	0.16	0.18	0.24	0.25	0.16	0.17
H3	0.15	0.09	0.13	0.13	0.18	0.18	0.15	0.18	0.22	0.25	0.16	0.16
N4	−0.25	−0.09	−0.11	0.12	−0.61	−0.34	−0.68	−0.37	−0.20	−0.03	−0.67	−0.43
H5	0.23	0.17	0.16	0.09	0.40	0.37	0.41	0.41	0.40	0.39	0.42	0.41
Cl6	−0.16	−0.72	−0.16	−0.75	−0.16	−0.65	−0.07	−0.62	−0.20	−0.65	−0.08	−0.49
C7	0.39	0.55	0.47	0.62	0.79	0.84	0.75	0.76	0.36	0.36	0.76	0.77
O8	−0.61	−0.32	−0.64	−0.36	−0.79	−0.65	−0.75	−0.63	−0.61	−0.45	−0.77	−0.66
O9	−0.59	−0.31	−0.62	−0.35	−0.77	−0.63	−0.74	−0.61	−0.58	−0.46	−0.75	−0.65
$\sum CO_2$[a]	−0.81	−0.08	−0.79	−0.09	−0.77	−0.44	−0.74	−0.48	−0.83	−0.55	−0.76	−0.54

[a] $\sum CO_2$ = C7 + O8 + O9.

TABLE 10: Net Atomic Charges for I and TS in the First Triplet State

	AM1		PM3		HF/4-31G		HF/6-31G*		HF/6-311+G*		MP2/6-31G*	
	I	TS	**I**	TS	**I**	TS	**I**	TS	**1**	TS	**I**	TS
Cl	−0.34	−0.45	−0.44	−0.66	−0.28	−0.04	−0.28	−0.10	−0.65	−0.50	−0.28	−0.08
H2	0.17	0.18	0.16	0.19	0.20	0.20	0.19	0.21	0.26	0.27	0.19	0.18
H3	0.17	0.11	0.16	0.19	0.20	0.20	0.19	0.21	0.26	0.26	0.19	0.28
N4	−0.09	−0.22	0.24	0.30	−0.37	−0.53	−0.39	−0.54	−0.03	−0.24	−0.40	−0.55
H5	0.25	0.23	0.12	0.12	0.38	0.32	0.41	0.35	0.40	0.33	0.42	0.36
Cl6	−0.37	−0.74	−0.49	−0.94	−0.36	−0.30	−0.39	−0.29	−0.43	−0.29	−0.38	−0.28
C7	0.40	0.54	0.49	0.60	0.77	0.61	0.74	0.49	0.36	0.08	0.77	0.49
O8	−0.60	−0.31	−0.63	−0.41	−0.79	−0.72	−0.75	−0.65	−0.61	−0.47	−0.77	−0.68
O9	−0.58	−0.32	−0.60	−0.39	−0.76	−0.75	−0.72	−0.68	−0.56	−0.45	−0.74	−0.72
$\sum CO_2$[a]	−0.78	−0.09	−0.74	−0.20	−0.78	−0.86	−0.73	−0.84	−0.81	−0.84	−0.74	−0.91

[a] $\sum CO_2$ = C7 + O8 + O9.

in this work: the specific details of the process may change if solvent effects and/or higher levels of theory (*e.g.*, CASSCF treatment) were included, but despite the main limitation of the calculations employed here, some important features could be clarified. The results can be summarized as follows:

(i) The energy of the PES for the triplet electronic state is higher than the energy for the PES of the singlet electronic state (except at the reactant zone when HF/4-31G calculations are carried out). The decomposition process is thus developed via the singlet electronic state.

(ii) The detailed analysis of the PES demonstrates that decomposition is a concerted process, in agreement with recent experimental results. The possible intermediates, *i.e.*, carbanion and nitrenium-like species, are not stationary points on the PES.

(iii) The TSs in singlet and triplet electronic states have antiperiplanar conformation, and this is not dependent on the method and basis set level used.

(iv) There are some differences between the results of semiempirical and *ab initio* procedures. The main differences are found in the activation energy and in the progress of the decomposition process. No relevant differences have been found between the use of the *ab initio* method at different basis set levels. Inclusion of correlation energy (MP2/6-31G*) has no effect on geometry for system **I**, but some differences have been found for TS.

(v) An analysis of Pauling bond orders shows that the process corresponds to a slightly asynchronous process. This agrees with experimental data. TS in the singlet electronic state presents the N4−Cl6 bond breaking more advanced than C1−C7 bond cleavage at the *ab initio* level, while an opposite effect is found if semiempirical methods are used. The TSs for singlet and triplet states are located in an advanced position along the reaction pathway, yielding a productlike character also in agreement with experimental data.

(vi) An analysis of charge distribution yields a continuous displacement of negative charge from carboxylate group to chlorine along the reaction pathway from **I** to TS.

Following our experimental/theoretical collaboration, we are now studying more complex *N*-chloro-α-amino acids in order to rationalize the substituent and kinetic isotope effects.

Acknowledgment. This work was supported by the Conselleria d'Educació i Ciència of the Generalitat Valenciana (Project GV-1142/93) and by DGICYT (Project PB93-0661). All calculations were performed on an IBM RS6000 workstation of the Departament de Ciències Experimentals of the Universitat Jaume I and on the cluster of Hewlett-Packard 9000/730 workstations of the Centre de Processament de Dades of the Universitat Jaume I. We are greatly indebted to these centers for providing us with computer capabilities.

References and Notes

(1) Owusu-Yaw, J.; Wheeler, W. B.; Wei, C. I. *Water Chlorination (Environmental Science and Technology)*; Lewis Publishers: Boca Raton, FL, 1990; Vol. 6, p 179.

(2) Franzén, R.; Kronberg, L. *Environ. Sci. Technol.* **1994**, *28*, 2222.

(3) Schonberg, A.; Moulbacher, R. *Chem. Rev.* **1952**, *50*, 261.

(4) Stambro, W. D.; Smith, W. D. *Environ. Sci. Technol.* **1979**, *13*, 446.

(5) Armesto, X. L.; Canle L., M.; Losada, M.; Santaballa, J. A. *J. Org. Chem.* **1994**, *59*, 4659.

(6) Hand, V. C.; Snyder, M. P.; Margerum, D. W. *J. Am. Chem. Soc.* **1983**, *105*, 4022.

(7) Awad, R.; Hussain, A.; Crooks, P. A. *J. Chem. Soc., Perkin Trans. 2* **1990**, 1233.

(8) Armesto, X. L.; Canle L., M.; Losada, M.; Santaballa, J. A. *Int. J. Chem. Kinet.* **1993**, *25*, 1.

(9) Armesto, X. L.; Canle L., M.; Losada, M.; Santaballa, J. A. *Int. J. Chem. Kinet.* **1993**, *25*, 331.

(10) Friedman, A. H.; Morgulis, S. *J. Am. Chem. Soc.* **1936**, *58*, 909.

(11) Ingols, R. S.; Wyckoff, H. A.; Kethley, T. W.; Hasdgen, H. W.; Fincher, E. L.; Webrand, J. C.; Mandl, J. E. *Ind. Eng. Chem.* **1953**, *45*, 996.

(12) Antelo, J. M.; Arce, F.; Franco, J.; Rodriguez, P.; Varela, A. *Int. J. Chem. Kinet.* **1988**, *20*, 433.

(13) Antelo, J. M.; Arce, F.; Crugeiras, J.; Franco, J.; Varela, A. *Int. J. Chem. Kinet.* **1990**, *22*, 1271.

(14) Glasstone, K. J.; Laidler, K. J.; Eyring, H. *The Theory of Rate Processes*; McGraw-Hill: New York, 1941.

(15) Laidler, K. J. *Theories of Chemical Reaction Rates*; McGraw-Hill: New York, 1969.
(16) Durán, M.; Bertrán, J. *Rep. Mol. Theory* **1990**, *1*, 57.
(17) Stanton, R. W.; McIver, Jr., J. V. *J. Am. Chem. Soc.* **1975**, *97*, 3632.
(18) Williams, I. H. *Chem. Soc. Rev.* **1993**, 277.
(19) Frisch, M. J.; Trucks, G. W.; Head-Gordon, M.; Gill, P. M. W.; Wong, M. W.; Foresman, J. B.; Johnson, B. G.; Schlegel, H. B.; Robb, M. A.; Replogle, E. S.; Gomperts, R.; Andres, J. L.; Raghavachari, K.; Binkley, J. S.; Gonzalez, C.; Martin, R. L.; Fox, D. J.; Defrees, D. J.; Baker, J.; Stewart, J. J. P.; Pople, J. A. *GAUSSIAN92, Revision A*; Gaussian Inc.: Pittsburgh, PA, 1992.
(20) Stewart, J. J. P. *J. Comput. Chem.* **1989**, *10*, 209.
(21) Stewart, J. J. P. *J. Comput. Chem.* **1989**, *10*, 221.
(22) Dewar, M. J. S.; Zoebisch, E. G.; Healy, E. F.; Stewart, J. J. P. *J. Am. Chem. Soc.* **1984**, *107*, 3902.
(23) Pople, J. A.; Beveridge, D. L.; Dobosh, P. A. *J. Chem. Phys.* **1967**, *47*, 2026.
(24) Stewart, J. J. P. In *Reviews in Computational Chemistry*; Lipkowitz, K. B., Boyd, D. B., VCH Publishers: New York, 1990; pp 45−81.
(25) Stewart, J. J. P. *J. Comput. Aided Mol. Des.* **1990**, *4*, 1.
(26) Stewart, J. J. P. *J. Comput. Chem.* **1990**, *11*, 543.
(27) Zerner, M. C. In *Reviews in Computational Chemistry*; Lipkowitz, K. B., Boyd, D. B., VCH Publishers: New York, 1991; Vol. 2, pp 313−365.
(28) Malwitz, N. *J. Phys. Chem.* **1995**, *99*, 5291−5298.
(29) Moller, C.; Plesset, M. S. *Phys. Rev.* **1934**, *46*, 618.
(30) Pople, J. A.; Nesbet, R. K. *J. Chem. Soc.* **1954**, 571.
(31) Roothaan, C. C. J. *Rev. Mod. Phys.* **1960**, *23*, 179.
(32) Jensen, J. H.; Gordon, M. S. *J. Am. Chem. Soc.* **1991**, *113*, 7917.
(33) Ramek, M.; Cheng, V. K. W.; Frey, R. F.; Newton, S. Q.; Schaefer, L. *J. Mol. Struct.* (*THEOCHEM*) **1991**, *1*, 235.
(34) Frey, R. F.; Coffin, J.; Newton, S. Q.; Ramek, M.; Cheng, V. K. W.; Momany, F. A.; Schaefer, L. *J. Am. Chem. Soc.* **1992**, *114*, 5369.
(35) Ding, Y.; Krogh-Jespersen, K. *Chem. Phys. Lett.* **1992**, *199*, 261.
(36) Ramek, M.; Cheng, V. K. W. *Int. J. Quantum Chem.* **1992**, *19*, 15.
(37) Schlegel, H. B. *J. Comput. Chem.* **1982**, *3*, 214.
(38) Schlegel, H. B. *J. Chem. Phys.* **1982**, *77*, 3676.
(39) Baker, J. *J. Comput. Chem.* **1986**, *7*, 385.
(40) Baker, J. *J. Comput. Chem.* **1987**, *8*, 563.
(41) Canle L., M. Doctoral Thesis, Universidade da Coruña, Spain, 1994.
(42) Bartlett, R. J. *Annu. Rev. Phys. Chem.* **1981**, *32*, 359.
(43) Bachrach, S. M. *J. Org. Chem.* **1994**, *59*, 5027.
(44) Pauling, L. *J. Am. Chem. Soc.* **1947**, *69*, 542.
(45) Grob, C. A.; Baumann, W. *Helv. Chim. Acta* **1955**, *38*, 594.
(46) Hehre, W. J.; Radom, L.; Schleyer, P. v. R.; Pople, J. A. *Ab Initio Molecular Orbital Theory*; John Wiley & Sons: New York, 1986.
(47) Otto, P.; Ladik, J. *Int. J. Quantum Chem.* **1980**, *18*, 1143.
(48) Mestres, J.; Durán, M.; Bertrán, J. *Theor. Chim. Acta* **1994**, *88*, 325.

JP9517209